Supplemental material

Juettner et al., https://doi.org/10.1083/jcb.201807210

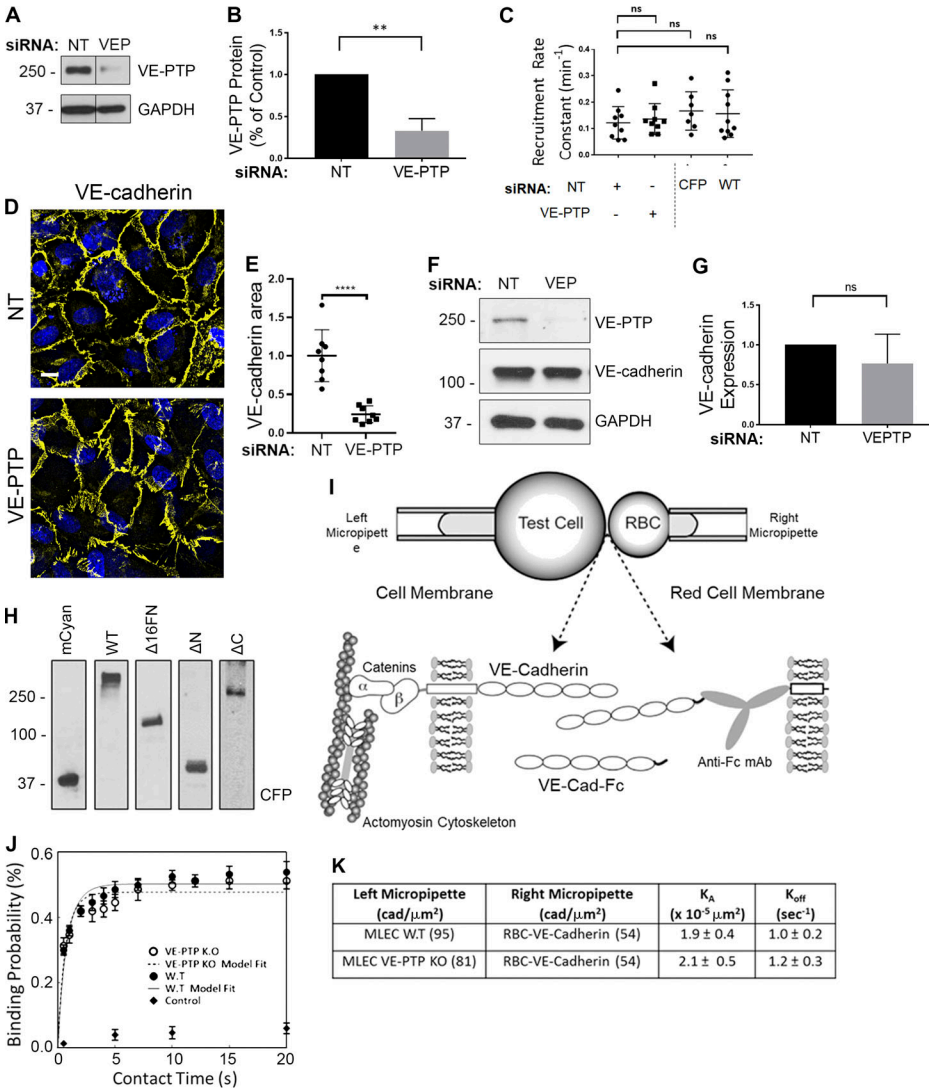

Left Micropipette (cad/μm²)	Right Micropipette (cad/μm²)	K_A (x 10^{-5} μm²)	K_{off} (sec^{-1})
MLEC W.T (95)	RBC-VE-Cadherin (54)	1.9 ± 0.4	1.0 ± 0.2
MLEC VE-PTP KO (81)	RBC-VE-Cadherin (54)	2.1 ± 0.5	1.2 ± 0.3

Figure S1. **VE-PTP stabilizes AJs by reducing the VE-cadherin internalization rate, but not via VE-cadherin recruitment or trans-dimerization, in the quiescent endothelium (related to Figs. 1 and 2). (A and B)** Western blot analysis of VE-PTP protein expression in HPAECs treated with NT and VE-PTP siRNA (A) and quantification normalized to GAPDH (loading control) in (B); mean ± SEM, $n = 3$; **, $P < 0.05$. **(C)** Recruitment rate constants of VE-cad-Dendra2 to AJs in HPAECs treated with NT or VE-PTP siRNA were 0.12 ± 0.02 min^{-1} and 0.13 ± 0.01 min^{-1} respectively; mean ± SEM; $n = 9$. Recruitment rate constants were 0.16 ± 0.02 s^{-1} and 0.15 ± 0.02 s^{-1} in control and WT VE-PTP–overexpressing cells; mean ± SEM; $n = 7–10$; unpaired t test. **(D)** Immunofluorescent images of VE-cadherin in confluent HPAEC monolayers treated with NT siRNA and VE-PTP siRNA. Scale bar, 10 µm. **(E)** Analysis of VE-cadherin junctional area from data in D; mean ± SEM; $n = 1$; ****, $P < 0.0001$, unpaired t test. **(F and G)** Western blot analysis of VE-cadherin protein expression in HPAECs treated with NT and VE-PTP siRNA (F) and quantification normalized to GAPDH (loading control; G). VE-cadherin level did not significantly change; $n = 3$, unpaired t test. **(H)** Western blot analysis of VE-PTP mutants; mCyan (control), full-length (WT) VE-PTP, Δ16FN VE-PTP (lacking FN1-16) mutant, ΔN VE-PTP (lacking extracellular domain), and ΔC VE-PTP (lacking cytosolic domain) mutants (as in Figs. 1 F and 2 A) overexpressed in HPAECs. **(I)** Schematic representation of micropipette experiments. **(J)** Binding probability of VE-cadherin trans-interaction in WT and VE-PTP knockout MLECs. RBCs without immobilized VE-cadherin-Fc served as control. The solid, dashed lines are weighted; nonlinear least squares fit of the data. **(K)** Table of VE-cadherin kinetics in WT and VE-PTP knockout ECs; $n = 54$ per group.

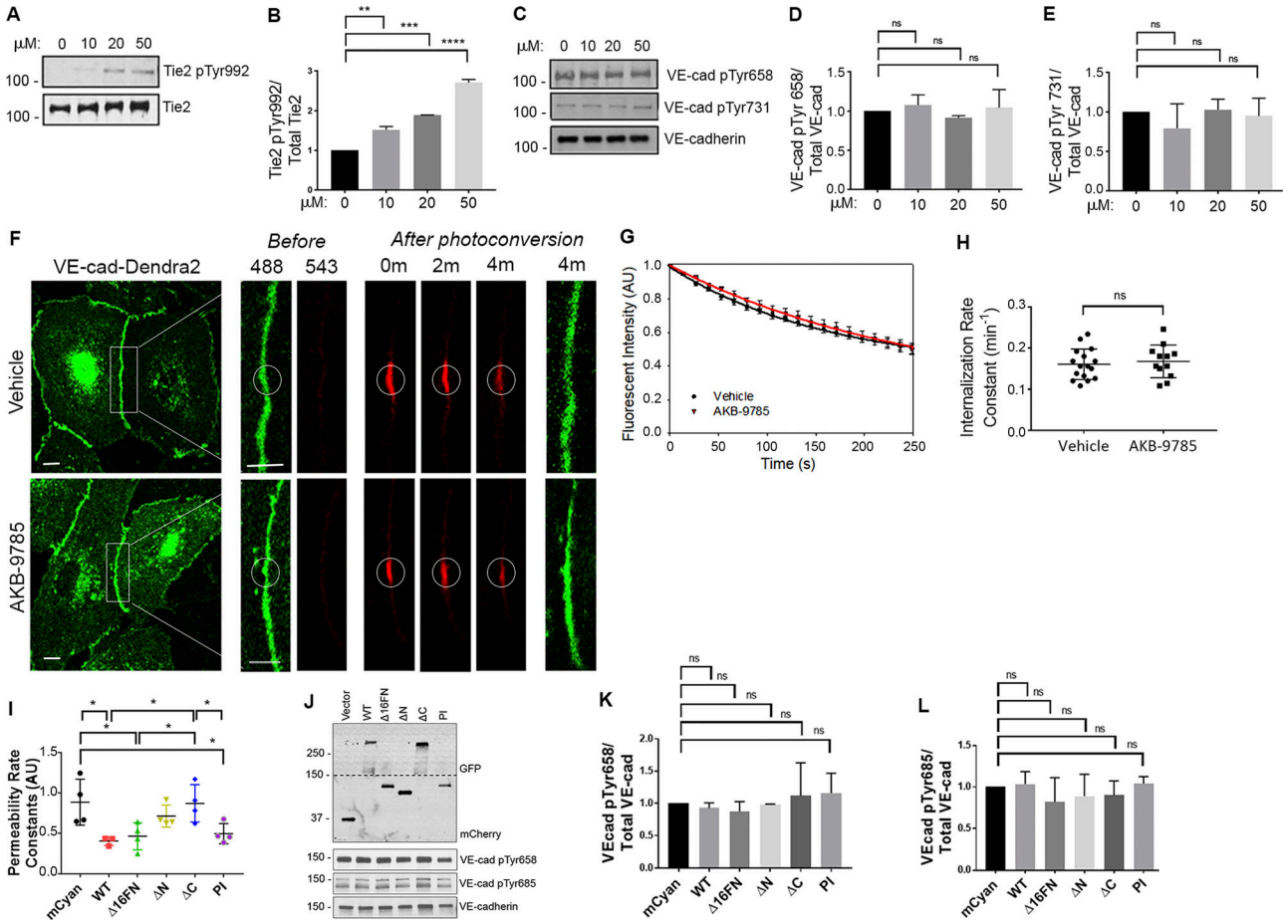

Figure S2. **Inhibition of VE-PTP phosphatase activity with AKB-9785 fails to prevent the VE-cadherin internalization rate at AJs (related to Figs. 1 and 2). (A–E)** Results of Western blot analyses of Tie-2 phosphorylation at Y992 and VE-cadherin phosphorylation at Y658 (VE-PTP dependent) and Y731 (VE-PTP independent; control) in HPAECs treated with indicated concentrations of AKB-9785. Inhibition of VE-PTP phosphatase activity with AKB-9785 increases Tie-2 tyrosine phosphorylation at Y992, consistent with Tie2 activation as previously described (Shen et al., 2014; Frye et al., 2015) but has no effect on VE-cadherin phosphorylation at selected tyrosine residues. Quantifications are shown in B, D, and E; mean ± SEM, $n = 2$; **, $P < 0.001$; ***, $P < 0.005$; ****, $P < 0.0001$; ns, not significant; one-way ANOVA. **(F)** Time-lapse images of VE-cad-Dendra2 in HPAECs treated with vehicle or 50 µM AKB-9785. Scale bars, 5 µm. **(G)** VE-cadherin internalization from AJs from data in E; mean ± SEM, $n = 12–16$. **(H)** Internalization rate constants calculated from F were 0.16 ± 0.01 min^{-1} and 0.17 ± 0.01 min^{-1} in vehicle and 50 µM AKB-9785 treated cells; mean ± SEM; $n = 12–16$; ns, not significant; unpaired *t* test. **(I)** Permeability rate constants of HPAEC monolayers overexpressing VE-PTP mutants shown in Figs. 1 F and 2 A to FITC-conjugated albumin tracer; mean ± SEM; $n = 3–4$; *, $P < 0.05$ by one-way ANOVA. **(J–L)** Effect of VE-PTP mutants shown in Figs. 1 F and 2 A on tyrosine phosphorylation of VE-cadherin overexpressed in CHO-K1 cells. Western blot analysis with abs against VE-cadherin, phospho-specific Y658 and Y685 VE-cadherin, GFP or mRFP for detection of CFP-tagged or plum-tagged VE-PTP mutants, respectively (J) and quantification (K-L); $n = 2$; ns, not significant; unpaired *t* test.

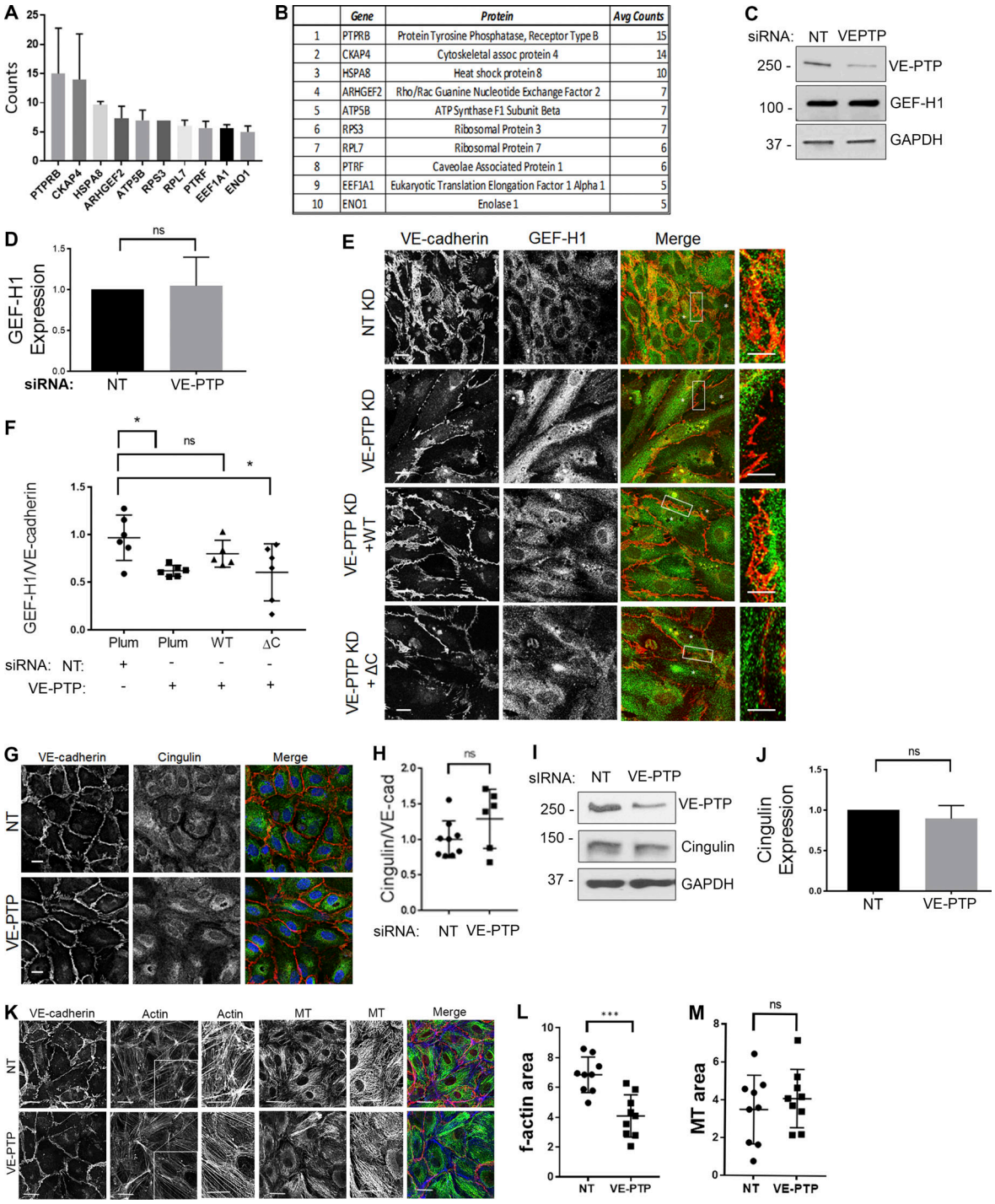

	Gene	Protein	Avg Counts
1	PTPRB	Protein Tyrosine Phosphatase, Receptor Type B	15
2	CKAP4	Cytoskeletal assoc protein 4	14
3	HSPA8	Heat shock protein 8	10
4	ARHGEF2	Rho/Rac Guanine Nucleotide Exchange Factor 2	7
5	ATP5B	ATP Synthase F1 Subunit Beta	7
6	RPS3	Ribosomal Protein 3	7
7	RPL7	Ribosomal Protein 7	6
8	PTRF	Caveolae Associated Protein 1	6
9	EEF1A1	Eukaryotic Translation Elongation Factor 1 Alpha 1	5
10	ENO1	Enolase 1	5

Figure S3. **VE-PTP binds GEF-H1 and stabilizes VE-cadherin junctions (related to Figs. 3 and 4). (A)** The histogram demonstrating abundance of unique peptides found by mass spectrometry. Gene names are indicated. The number of counts is shown on the bars. See Materials and methods for more details. **(B)** Table of unique peptides found by mass spectrometry with corresponding gene and protein names. Myosin, an apparent VE-PTP–binding protein, is excluded from analysis. **(C and D)** Western blot analysis of GEF-H1 expression in HPAECs treated with NT siRNA or VE-PTP siRNA (GAPDH was used as a loading control; C) and data quantification (D); *n* = 3, unpaired *t* test. **(E)** Immunofluorescent images of VE-cadherin (red) and GEF-H1 (red) in confluent HPAEC monolayers treated with NT siRNA or VE-PTP siRNA and overexpressing mCyan (vector control), VE-PTP WT, or VE-PTP ΔC. Asterisk (*) denotes transfected cells. Scale bars, 10 µm. **(F)** Analysis of GEF-H1 expression at VE-cadherin junctions from data in E; mean ± SEM; *n* = 5–6 images per group; one-way ANOVA; $P < 0.05$. **(G and H)** Immunofluorescent staining for VE-cadherin (red) and cingulin (green) in HPAECs treated with NT siRNA or VE-PTP siRNA (G) and data quantification (H). Scale bar, 10 µm. *n* = 6–8 fields from three independent experiments; unpaired *t* test. **(I and J)** Western blot analysis of cingulin in HPAECs treated with NT siRNA or VE-PTP siRNA (GAPDH was used as a loading control; I) and data quantification (J); mean ± SEM; *n* = 3; unpaired *t* test. **(K)** Immunofluorescent staining for VE-cadherin (red), actin (blue), and microtubules (green) in HPAECs treated with NT siRNA or VE-PTP siRNA. Scale bars, 10 µm. **(L and M)** Analysis of F-actin (L) and microtubule (M) areas normalized to the cell area; mean ± SEM; *n* = 18 images from two independent experiments; ***, $P < 0.001$; unpaired *t* test. Scale bar, 10 µm.

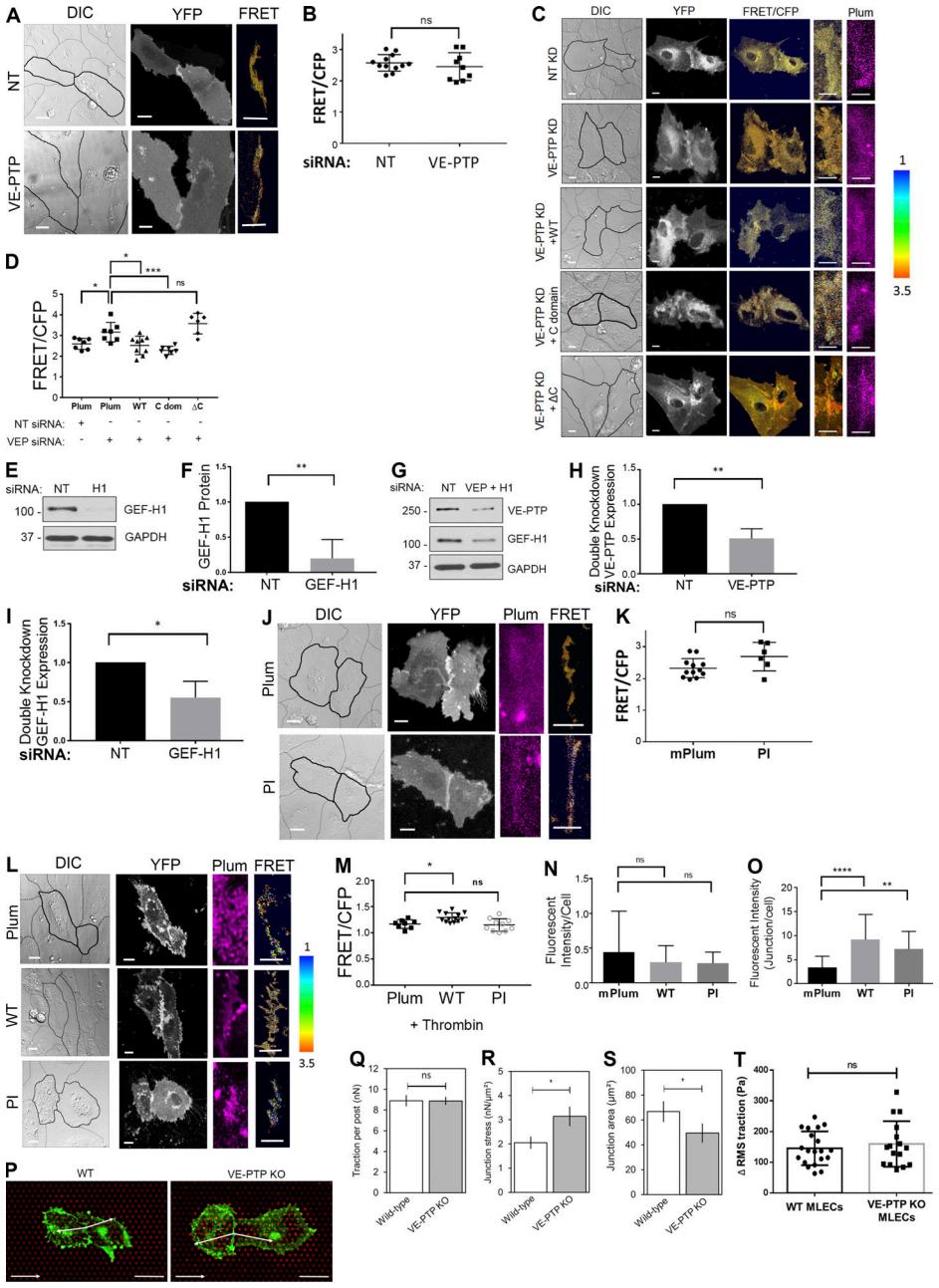

Figure S4. **VE-PTP relieves tension across VE-cadherin junctions by inhibiting RhoA signaling (related to to Figs. 4 and 5). (A and B)** Rac1 activity images and quantification at VE-cadherin junctions in HPAECs treated with NT or VE-PTP siRNA. Scale bars, 5 µm. *n* = 3, unpaired *t* test. **(C)** RhoA FRET of HPAECs in confluent monolayers treated with NT siRNA or VE-PTP siRNA and overexpressing mCyan (control), VE-PTP WT, VE-PTP C domain, or VE-PTP ΔC. Scale bars, 5 µm. **(D)** Quantification of data in A; *n* = 6–9 junctions from two independent experiments. *, P < 0.05; ***, P < 0.0001; unpaired *t* test. **(E–I)** Western blot analyses of VE-PTP and GEF-H1 expression in HPAECs treated with NT siRNA, GEF-H1 siRNA, or VE-PTP and GEF-H1 siRNA; GAPDH, loading control. (F and H–I) Quantification of data in B and D; mean ± SEM; *n* = 3; *, P < 0.05; **, P < 0.001; unpaired *t* test. **(J and K)** Rac1 activity at VE-cadherin junctions in HPAECs overexpressing mPlum or Plum-VE-PTP PI; *n* = 6–10 junctions from two independent experiments; unpaired *t* test. **(L and M)** Tension across VE-cadherin junctions in HPAECs overexpressing mPlum, mPlum-VE-PTP (WT), or mPlum-VE-PTP PI (PI) and treated with 50 nM human α-thrombin for 15 min. DIC, VE-cadherin tension biosensor (YFP), VE-PTP (magenta), and FRET/CFP (color-coded) images are shown (L). The ratiometric images scaled from 1 to 3.5 and color-coded as indicated on the right; warmer colors denote low tension. Scale bars, 5 µm. (M) Quantification of data in H; *n* = 8–12 junctions from three independent experiments; *, P < 0.05; one-way ANOVA. **(N and O)** Expression levels of mPlum, WT, or PI in HPAECs used in FRET studies. Fluorescence intensity per cell (N) and at the junction normalized to total mPlum fluorescence (O); *n* = 21–32 from nine experiments; **, P < 0.001; ****, P < 0.0001; one-way ANOVA. **(P)** Stress at AJs determined by micropillar array assay. Fluorescent images of WT (*VE-PTP*$^{flox/flox}$) and VE-PTP KO MLECs grown on fibronectin-coated micropillar posts (red). Junctions were visualized with β-catenin staining (green). Sum of traction forces shown by vectors (see Materials and methods). Scale bars, 30 µm; force bars, 100 nN. **(Q–S)** Quantification of junction stress, area, and traction. VE-PTP knockout mouse cells show increased junctional stress and reduced junctional area. *n* = 12–14. Stress values were 2.05 ± 0.25 nN/µm² and 3.13 ± 0.40 nN/µm in WT and VE-PTP KO MLEC; mean ± SEM; *, P < 0.05 by unpaired *t* test. **(T)** Bar graph indicating traction changes (ΔRMS traction, Pa) exerted by WT MLECs and VE-PTP KO MLECs plated on 40-kPa gels coated with fibronectin (*n* = 20 for WT MLECs and *n* = 16 for VE-PTP KO MLECs). A two-tailed *t* test showed no significant differences.

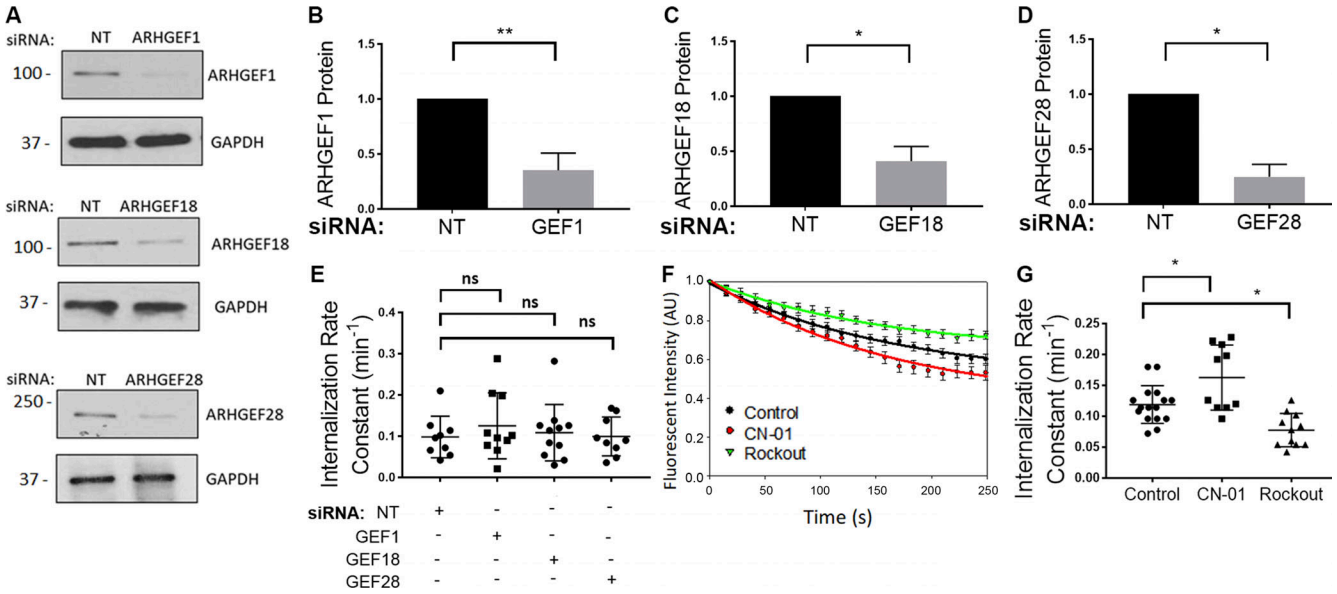

Figure S5. **Relative contributions of RhoGEFs and Rho signaling in regulating the VE-cadherin internalization rate. (A–D)** Western blot analysis (A) and data quantification (B–D) of ARHGEF1, ARHGEF18, and ARHGEF28 in HPAECs depleted of these proteins, n = 2–3; *, P < 0.05; **, P < 0.001, unpaired t test. **(E)** VE-cad-Dendra2 internalization rate constants in HPAEC monolayers treated as indicated; mean ± SEM; n = 9–11 junctions from three independent experiments; one-way ANOVA. **(F and G)** Effect of Rho signaling on the VE-cadherin internalization rate at AJs. VE-cad-Dendra2 internalization curves (F) and internalization rate constants (G) in HPAECs treated with vehicle, 50 µM Rho activator (CN-01), or 50 µM ROCK inhibitor (Rockout); mean ± SEM; n = 8–16 junctions from three independent experiments; *, P < 0.05; one-way ANOVA.

References

Frye, M., M. Dierkes, V. Küppers, M. Vockel, J. Tomm, D. Zeuschner, J. Rossaint, A. Zarbock, G.Y. Koh, K. Peters, et al. 2015. Interfering with VE-PTP stabilizes endothelial junctions in vivo via Tie-2 in the absence of VE-cadherin. *J. Exp. Med.* 212:2267–2287. https://doi.org/10.1084/jem.20150718

Shen, J., M. Frye, B.L. Lee, J.L. Reinardy, J.M. McClung, K. Ding, M. Kojima, H. Xia, C. Seidel, R. Lima e Silva, et al. 2014. Targeting VE-PTP activates TIE2 and stabilizes the ocular vasculature. *J. Clin. Invest.* 124:4564–4576. https://doi.org/10.1172/JCI74527